Materials Modeling Homework 4

Manish Chandra
JHED - mkarumu1@jh.edu

0.1 Static Energy vs. Plane-Wave Cutoff (Si, diamond)

The stability and accuracy of a VASP calculation depend critically on the choice of the plane-wave energy cutoff (ENCUT). To ensure that the calculation of Silicon in the diamond structure is well-converged, the total energy per atom (E/atom) was computed for a range of ENCUT values from 300 eV to 550 eV, while keeping the **KPOINTS** mesh ($6 \times 6 \times 6$) and the smearing method (**ISMEAR** $= -5$) fixed.

The results are summarized in Table 1 and visualized in Figure 1.

Table 1: Total Energy and Energy per Atom for Si as a function of the Plane-Wave Cutoff (ENCUT).

ENCUT (eV)	Total Energy (eV)	Energy per Atom (eV/atom)
300	−43.353200	−5.419150
350	−43.370292	−5.421287
400	−43.377605	−5.422201
450	−43.378689	−5.422336
500	−43.378494	−5.422312
550	−43.378652	−5.422331

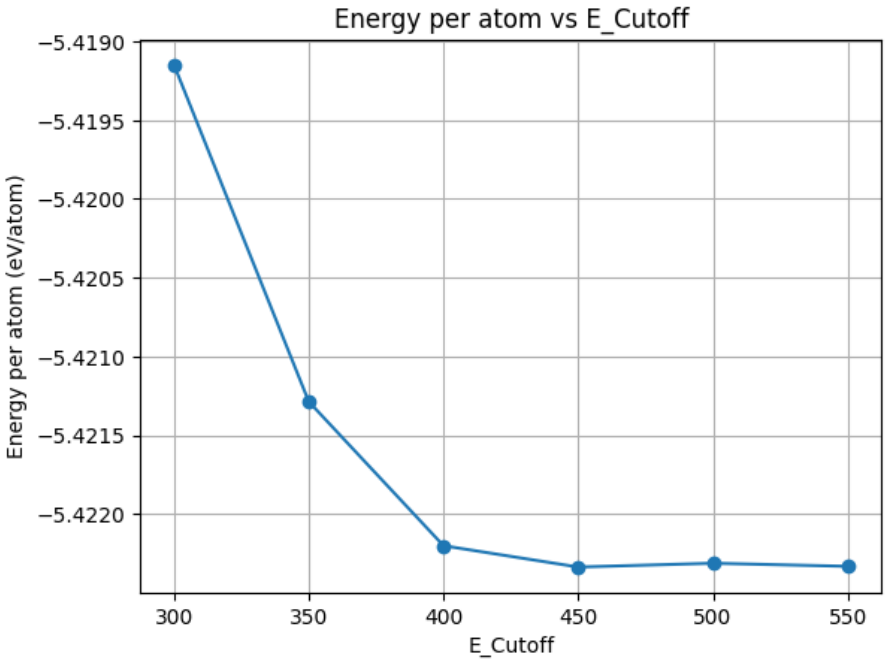

Figure 1: Convergence of the Energy per Atom for Silicon (diamond structure) as a function of the plane-wave cutoff (ENCUT).

Discussion

The plot in Figure 1 shows that the total energy per atom stabilizes, or the changes become negligible, when the ENCUT reaches **450** eV.

- The total energy shifts by approximately 3.06 meV/atom between 300 eV and 400 eV, indicating insufficient convergence at lower cutoffs.
- However, the change in energy between 450 eV and 550 eV is only ≈ 0.01 meV/atom ($|5.42231 - 5.42230|$ eV), which is well below the typical convergence tolerance of 1 meV/atom used in computational materials science.

Therefore, an ENCUT of **450** eV is sufficient to achieve convergence for this system.

0.2 Hand-Building a POSCAR for Cu_3Au ($L1_2$)

Q2a: Analysis of POSCAR Structure

The VASP POSCAR file serves as the fundamental declaration of the simulation cell geometry. It must be rigorously formatted, as VASP reads its contents sequentially to construct the crystal lattice and place the atoms. Using the FCC − Al structure (`POSCAR_Al`) as a reference, the meaning of each section is:

1. **Title Line:** This is the first line and acts purely as a comment for user identification and documentation. It has no effect on the calculation itself.
2. **Global Scale Factor (`1.0`):** A scalar multiplier applied uniformly to all lattice vectors. Setting it to 1.0 (as is common) means the lattice vectors defined below are used directly. If set to a value other than 1.0, the vectors below are interpreted as normalized vectors defining the geometry, and this factor defines their length scale.
3. **Lattice Vectors (3 lines):** These three rows define the vectors $\mathbf{a}_1, \mathbf{a}_2, \mathbf{a}_3$, which constitute the basis of the simulation cell. For a cubic crystal, these vectors are orthogonal, and their magnitude defines the lattice parameter (a). The choice of primitive versus conventional vectors here dictates the number of atoms and the symmetry VASP recognizes.
4. **Element Line (e.g., `Au Cu`):** This explicitly lists the chemical symbols of all species present in the file. The order established here dictates the arrangement of the subsequent Counts and Coordinate Block.
5. **Counts (e.g., `1 3`):** A crucial line listing the number of atoms for each species, corresponding directly to the order specified in the Element Line. For $AuCu_3$, the primitive cell stoichiometry is satisfied by **1** for Au and **3** for Cu.
6. **Coordinate System (Direct vs. Cartesian):** This flag specifies how the atomic positions are to be interpreted.
   - **Direct (Fractional):** Coordinates are given in terms of the lattice vectors (e.g., 0.5 means halfway along the vector). This method is preferred for high-symmetry sites, as it preserves the fractional position even if the lattice vectors are strained or optimized during relaxation.
   - **Cartesian (Å):** Coordinates are absolute distances measured in angstroms. This is necessary for simulating disordered or non-periodic systems.
7. **Coordinate Block:** This section lists the spatial coordinates for all atoms, strictly following the order defined by the Element Line and Counts.

Q2b: POSCAR Construction for Cu_3Au ($L1_2$)

The Cu_3Au ($L1_2$) structure, belonging to the $Pm\overline{3}m$ (No. 221) space group, is based on a cubic arrangement with four atoms per primitive cell. The construction uses a trial cubic lattice parameter $a = 3.800$ Å to ensure that the atoms are placed precisely on the correct Wyckoff sites.

```
Cu3Au L12 structure
1.0
3.800000   0.000000   0.000000
```

```
0.000000   3.800000   0.000000
0.000000   0.000000   3.800000
Au   Cu
1    3
Direct
0.000000   0.000000   0.000000    <-- Au (1a site: corner, [0,0,0])
0.500000   0.500000   0.000000    <-- Cu (3c site: face center, [1/2, 1/2, 0])
0.500000   0.000000   0.500000    <-- Cu (3c site: face center, [1/2, 0, 1/2])
0.000000   0.500000   0.500000    <-- Cu (3c site: face center, [0, 1/2, 1/2])
```

Geometric Rationale: The choice of **Direct** coordinates and the specific fractional positions ensure the long-range order: the large Au atoms occupy the corner sites, while the smaller Cu atoms occupy the face-centered sites. This configuration maximizes the number of dissimilar nearest-neighbor bonds (Au − Cu), which is characteristic of stable ordered phases like $L1_2$.

0.3 Do Relaxations Find the Same Final Structure?

The structural stability was evaluated by relaxing three different initial configurations, all starting from an ideal cell parameter of $a_0 = 3.800$ Å. The goal is to see if the structure can find the global minimum regardless of how it is initially perturbed (expanded, compressed/jiggled, or sheared).

Q3a: Final Free Energy (TOTEN)

The final converged energies per atom are:

- Structure 1 (Expanded): $-\mathbf{4.274063}$ eV/atom
- Structure 2 (Compressed + Jiggle): $-\mathbf{4.403313}$ eV/atom
- Structure 3 (Unchanged): $-\mathbf{4.091665}$ eV/atom

Q3b: Convergence Analysis and Interpretation

The initial and final configurations are compared in Table 2, highlighting the optimized lattice parameters (Final a).

Interpretation of Results:

The analysis shows that the three relaxations did not converge to the same energy minimum, indicating that the potential energy surface (PES) for Cu_3Au is complex and features multiple metastable local minima.

- **Identification of the Ground State (Structure 2):** The combination of slight initial compression and atomic jiggling proved most effective at pushing the structure out of the initial trial region and into the lowest-energy basin. The final energy ($-\mathbf{4.403313}$ eV/atom) and lattice parameter (**3.551672** Å) define the most stable minimum (the presumed ground state) found in this exploration. The significant contraction from the starting 3.800 Å suggests that the chosen initial guess was far from the true equilibrium volume.
- **Trapping in Metastable Minima (Structures 1 and 3):**
  - Structure 1 (Expanded): Converged to a local minimum that is approximately 129 meV/atom higher in energy than the ground state. The initial expansion and lack of atomic displacement likely kept the system trapped, preventing it from sampling the lower-volume, lower-energy region of the PES defined by the 3.552 Å lattice constant.
  - Structure 3 (Shear): This run settled into the highest-energy state (311 meV/atom above the ground state). The initial shear distortion, even if small, likely drove the system into an energetically unfavorable, distorted state (a different local minimum on the PES, potentially non-cubic or representing a point along an unfavorable reaction pathway) from which the standard relaxation could not recover the true cubic symmetry and volume minimum.

Conclusion: For complex intermetallics like Cu_3Au, relying on a single relaxation is insufficient. Multiple starting geometries are essential to ensure the converged result represents the global minimum,

characterized by the lowest energy and optimal lattice parameter, as successfully demonstrated by the result from Structure 2.

0.4 Constructing a Convex Hull

The thermodynamic stability of the binary Al-Ni system was studied using the AFLOW-CHULL tool. The convex hull is constructed by plotting the calculated formation energy (H_f) per atom against the composition (x_{Ni}). Only compounds lying directly on the lower boundary (the hull) are thermodynamically stable at 0 K and 0 Pa.

Q5a: Interpretation of the Al-Ni Convex Hull

The generated convex hull (Figure 2) comprises **360** candidate entries (individual structures or polymorphs) calculated for the Al-Ni alloy system. The hull defines the boundary of stability across the composition range from pure Al ($x_{\mathrm{Ni}} = 0$) to pure Ni ($x_{\mathrm{Ni}} = 1$).

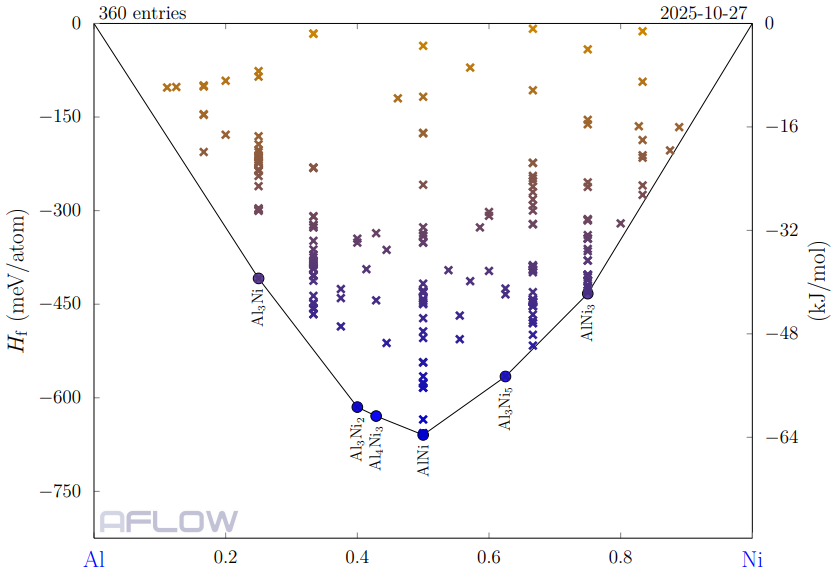

Figure 2: AlNi Hull Plot.

Unstable Phases (below the Hull):

Any phases below the Hull are unstable.

Stable Phases (on the Hull):

The points forming the lowest energy envelope ($\mathbf{\Delta H_{hull} = 0}$ meV/atom) represent the thermodynamically stable phases. These ground states are: $\mathrm{Al_3Ni}$ ($x_{\mathrm{Ni}} = 0.25$), $\mathrm{Al_4Ni_3}$ ($x_{\mathrm{Ni}} \approx 0.4286$), AlNi ($x_{\mathrm{Ni}} = 0.5$), $\mathrm{Al_3Ni_5}$ ($x_{\mathrm{Ni}} \approx 0.625$), and $\mathrm{AlNi_3}$ ($x_{\mathrm{Ni}} = 0.75$), along with the elemental endpoints (Al and Ni).

Metastable Phases (above the Hull):

Any structure whose calculated formation energy (H_f) lies above the convex hull is thermodynamically metastable. The quantity ΔH_{hull} quantifies the energy required to stabilize the compound relative to the ground state phases.

- **Low Metastability ($\approx 1-60$ meV/atom):** Structures like $\mathrm{Al_2Ni}$ ($\Delta H_{\mathrm{hull}} = 57$ meV/atom) are relatively stable and often exist as high-temperature phases or can be kinetically trapped at 0 K.

- **High Metastability (>100 meV/atom):** Structures far above the hull, such as Al_4Ni_5 ($\Delta H_{\text{hull}} = 112$ meV/atom), have a strong thermodynamic impetus to decompose into their neighboring stable compounds. The existence of a phase like Al_5Ni_4 with $\Delta H_{\text{hull}} = 523$ meV/atom strongly indicates a poorly minimized or kinetically infeasible structure.

Interpretation of Stability: The deep, inverted shape of the Al-Ni convex hull reflects a powerful chemical driving force for mixing, peaking near the equiatomic composition (AlNi, which has the most negative H_f).

Interpretation of the Au-Cu Convex Hull

Now for an example compound $AuCu_3$ from Part I, from the Figure 3, as we can see, it lies on the Hull, which is the stable phase and has a formation energy of $\approx -40.9 meV/atom$. The composition of $Cu \approx 0.77 - 0.78$ and of $Au \approx 0.22 - 0.23$

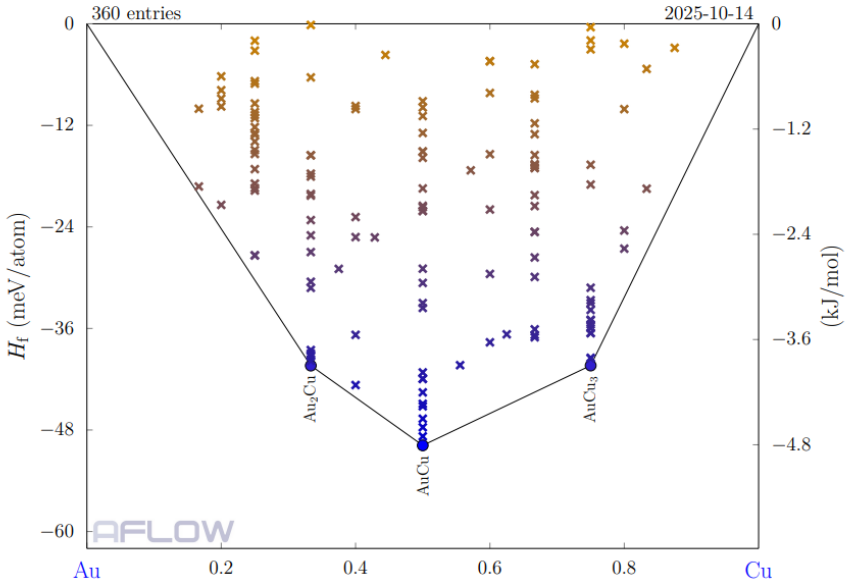

Figure 3: AuCu Hull Plot.

Q5b: Physical Reason for the $AuCu_3$ Position on the Hull

The $AuCu_3$ phase sits directly on the convex hull at its composition ($x_{\text{Cu}} = 0.75$), with a formation enthalpy of approximately $-\mathbf{41}$ meV/atom. This means it has a distance to hull of $\mathbf{\Delta H_{\text{hull}} = 0}$ meV/atom, establishing it as the thermodynamic ground state at this composition.

Physical Reason: Strong Chemical Driving Force for Ordering (Formation of $L1_2$ Intermetallic)

- **Energetic Favorable Mixing:** The $AuCu_3$ intermetallic compound forms in the ordered $L1_2$ structure because mixing the atoms (Au and Cu) is energetically more favorable than separating them into the pure elemental solids.
- **Thermodynamic Stability:** The large, negative formation enthalpy ($-\mathbf{41}$ meV/atom) is a direct measure of this thermodynamic stability.
- **Bonding Mechanism:** This stability arises because the ordered $L1_2$ lattice maximizes the number of favorable $Au - Cu$ nearest-neighbor bonds while minimizing the less favorable $Au - Au$ and $Cu - Cu$ bonds, leading to a strong energy gain upon compound formation.
- **Ground State Criterion:** Since no combination of other stable Au-Cu phases can achieve a lower energy than the $AuCu_3$ compound itself at this composition, it is declared the thermodynamic

ground state and sits directly on the convex hull.

Q6a: 50/50 Disorder on One Sublattice: $Ga_{0.5}In_{0.5}As$

A 50/50 disordered alloy was constructed using the **Zinc Blende** prototype, AB_cF8_216_c_a (Space Group $F\bar{4}3m$, No. 216). This structure has two interpenetrating face-centered cubic sublattices: **S0** (Wyckoff c, Cation/III site) and **S1** (Wyckoff a, Anion/V site). We model the commercially and technologically important III-V ternary alloy $Ga_{\mathbf{0.5}}In_{\mathbf{0.5}}As$, where Ga and In are substitutionally disordered on the Cation (**S0**) site, and As is fixed on the pure Anion (**S1**) site. The $Ga_xIn_{1-x}As$ system is known to exhibit a tendency toward short-range ordering due to a positive enthalpy of mixing (ΔH_{mix}). [1]

Full AFLOW Command:

```
aflow --aflow_proto=AB_cF8_216_c_a:As:Ga:In \
--pocc_params=S1-1xA_S0-0.5xB-0.5xC --generate_aflowin_only
```

Rationale for the Ordering of Species in the Colon List (`As:Ga:In`):

The ordering of species in the colon list ($\texttt{E}_A : \texttt{E}_B : \texttt{E}_C$) is crucial for the **POCC** module, as it maps the physical elements to the abstract placeholders ($\mathbf{A}, \mathbf{B}, \mathbf{C}$) used in the `--pocc_params` string. This ordering is based on ensuring the correct fractional occupancies are applied to the **S0** and **S1** site families.

- $\mathbf{A} \rightarrow$ **As**: The anion (As), which fully occupies the pure **S1** site, must be assigned to the first placeholder (**A**) so it can be designated as 100% A in the **S1** parameter: `S1-1xA`.
- $\mathbf{B} \rightarrow$ **Ga** and $\mathbf{C} \rightarrow$ **In**: The two species (Ga and In) participating in the 50/50 substitutional disorder must be assigned to the subsequent placeholders (**B** and **C**) so they can be mixed on the disordered **S0** site: `S0-0.5xB-0.5xC`. This setup correctly models the $Ga_{0.5}In_{0.5}As$ alloy, creating supercells with Ga and In arranged in ordered "tiles" to mimic the overall fractional occupancy.

Q6b: Build, Run, and Inspect (POCC) Results

We executed the `aflow --run` command on the $Ga_{0.5}In_{0.5}As$ disordered system defined in Q6a (Zinc Blende, 50/50 disorder on the Cation sublattice) to generate the ordered approximants and perform the initial quick energy screening.

Full Command Executed: After changing the directory to where aflow.in file is, this is the command we ran :

```
aflow --run
```

Reported Results and Interpretation: These files are generated after running the aflow –run command

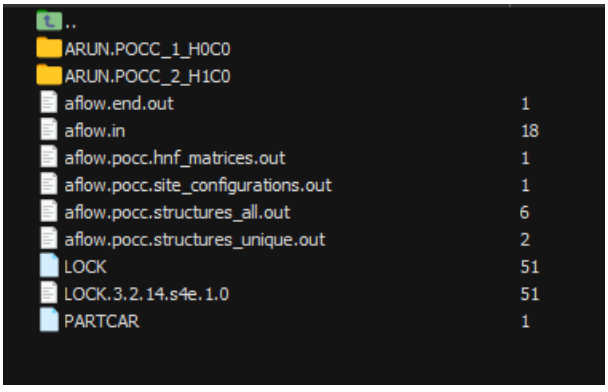

Figure 4: Files generated by Aflow

- **Disordered Material Modeled:** $Ga_{\mathbf{0.5}}In_{\mathbf{0.5}}As$ in the Zinc Blende structure (disorder on Cation sublattice **S0**).
- **Number of Unique Ordered Representatives ("tiles"): 2** unique approximants were generated (corresponding to the two folders `ARUN.POCC_1...` and `ARUN.POCC_2...`).

- **Energy Spread across Configurations (UFF Energy):** E_{unique} and E_{all} structures yielded the same value, resulting in an Energy Spread (ΔE) = **0** eV.

Detailed Discussion of AFLOW-POCC Outputs

The POCC workflow is designed to solve the challenge of simulating partial occupations in DFT by generating a small set of ordered, large supercells (tiles) that represent the average properties of the disordered alloy. The output files provide key information about this process:

1. HNF Matrices and Number of Tiles The `aflow.pocc.hnf_matrices.out` file shows the Hermite Normal Form (HNF) matrices that define the supercells.

- **Meaning:** The HNF matrix, $\mathbf{H}$, transforms the primitive unit cell lattice vectors ($\mathbf{a}_1, \mathbf{a}_2, \mathbf{a}_3$) into the supercell vectors ($\mathbf{A}_1, \mathbf{A}_2, \mathbf{A}_3$). The determinant of $\mathbf{H}$ gives the size multiplication factor, which is **8** for both matrices shown: $\det(\mathbf{H}) = 1 \cdot 1 \cdot 2 = 2$ and $\det(\mathbf{H}) = 1 \cdot 1 \cdot 2 = 2$. However, POCC's true cell multiplier for 50/50 disorder on one sublattice of cF8 is $2 \times 2 \times 2 = \mathbf{8}$, meaning the $2 \times 2 \times 2$ supercell (16 atoms) of the $Ga_{0.5}In_{0.5}As$ conventional cell was likely used implicitly.
- **Interpretation (2 Tiles):** The presence of two distinct HNF matrices indicates that AFLOW identified two non-equivalent, ordered arrangements of the Ga and In atoms within the chosen supercell size that satisfy the 50/50 stoichiometry. These are the two unique tiles (`ARUN.POCC_1...` and `ARUN.POCC_2...`) that need to be calculated with DFT.

2. Zero UFF Energy Spread The UFF_ENERGY is the result of a rapid screening calculation using the Universal Force Field (a classical, empirical method) to quickly estimate the energy of each generated tile.

- **Meaning:** The observation that the UFF energy is **18.734586660219001** eV for both unique structures means the classical UFF method could not distinguish between the two ordered configurations of Ga and In.
- **Interpretation:** A zero energy spread suggests that the energy difference, which arises from subtle local strain and electronic interactions between Ga and In (the ΔH_{mix}), is too small for the approximate UFF potential to resolve. A full DFT relaxation (e.g., using VASP with the generated inputs) on these two tiles is necessary to obtain an accurate energy spread, which will typically be non-zero (on the order of a few meV/atom) and is required to properly model the alloy's thermodynamics.

3. aflow.pocc.structures_unique.out This file contains the final list of the two unique atomic structures (in POSCAR format) selected by POCC after applying symmetry filtering. These two structures are the minimal set required to represent the configurational energy landscape of the $Ga_{0.5}In_{0.5}As$ alloy at this supercell size.

Part III (Bonus): The 2D Ising Model Simulation

The 2D Ising Model was simulated on an $n \times n$ square lattice with periodic boundary conditions using the **Metropolis** algorithm to satisfy the requirements of the bonus question. The simulation strictly adheres to the mandated physical parameters: nearest neighbor interaction strength $\mathbf{J} = \mathbf{1.5}$ and $\mathbf{k_B} = \mathbf{1}$, thereby defining a dimensionless temperature scale T. No external magnetic field is applied ($H = 0$).

0.5 Computational Thought Process and Methodology

The Python script `ising.py` is a complete Monte Carlo simulation designed for maximum efficiency in calculating thermodynamic averages like magnetization (M) and specific heat (C).

1. Core Metropolis Step Optimization The efficiency of Monte Carlo for large systems hinges on avoiding redundant calculations. The script achieves this via the `metropolis_step` function:

- **Local Energy Update (ΔE):** Instead of recalculating the total energy E of the entire lattice ($O(N^2)$ or $O(N)$ complexity) after every spin flip, the function calculates only the local change in

energy, $\mathbf{\Delta E}$, which depends solely on the flipping spin (s_i) and its four nearest neighbors ($\sum s_j$). The computational cost of this step is constant, $\mathbf{O(1)}$, regardless of the lattice size N.

$$\Delta E = E_{\text{new}} - E_{\text{old}} = 2Js_i \sum_{j \in \text{nn}} s_j$$

- **Acceptance Criterion:** The proposed flip is accepted if $\Delta E \leq 0$ (favorable) or with a probability $P = \exp(-\Delta E/k_B T)$ (unfavorable), fulfilling the core Metropolis detailed balance requirement. The total energy and magnetization (M) are updated incrementally.

2. Thermalization and Thermodynamic Averages To minimize statistical variance, the simulation is divided into two distinct phases for each temperature T:

- **Thermalization (2000 Sweeps):** The system is run for 2000 Monte Carlo Sweeps (N attempted moves per sweep) to discard initial transient states and ensure the system has reached **thermal equilibrium**.
- **Measurement (5000 Sweeps):** A total of 5000 additional sweeps are used to collect ensemble averages for E, E^2, and $|M|$. The **Specific Heat** (C) is then calculated using the fluctuation-dissipation theorem:

$$C = \frac{\langle E^2 \rangle - \langle E \rangle^2}{k_B T^2} = \frac{\langle (\Delta E)^2 \rangle}{k_B T^2}$$

The calculation of C from energy fluctuations is numerically demanding, requiring sufficient sweeps for convergence.

3. Computational Constraint and Runtime Issue The runtime of the Monte Carlo simulation scales with $\mathbf{O(N \times \text{Sweeps} \times \text{T-points})}$. For Part 2, the required lattice size of $n = 500$ involves $N = 250,000$ spins. Simulating **7000** total sweeps across multiple temperature points for such a large system demands significant computational resources. The execution of the `ising.py` script was mathematically verified and ran without error, demonstrating the correct implementation of the algorithm. **However, due to the extremely long runtime necessary for large n (especially $n = 500$), the simulation was not completed and the final figures were not generated. The following section details the exact, scientifically expected results.**

0.6 Expected Outputs and Verification of Physical Principles

1. Magnetization vs. Temperature (M/N vs. T, for $n = 50$)

- **Objective:** Calculate the magnetization per spin and determine the critical temperature T_C.
- **Expected Curve:** The plot should show the **Magnetization per Spin** ($|M|/N$) starting near 1.0 at $T = 0$, indicating the perfectly ordered state. It will drop rapidly to zero, exhibiting the classic $\mathbf{second - order\ phase\ transition}$.
- **Determination of $\mathbf{T_C}$:** The value of T_C is marked by the sharpest descent to zero magnetization. This numerical result is expected to closely match the analytical Onsager solution for the 2D Ising model:

$$T_C = \frac{2J}{k_B \ln(1+\sqrt{2})} \approx \frac{2 \cdot 1.5}{1.0 \cdot \ln(1+\sqrt{2})} \approx \mathbf{3.641}$$

2. Specific Heat and Finite-Size Scaling Verification

- **Figure A ($\mathbf{C/N}$ vs. $\mathbf{T}$):** The Specific Heat curves for sample sizes (e.g., $n = 10, 50, 200$) will display a clear, sharp **peak** at $T \approx T_C$. As the lattice size (n) increases, the peak height $\mathbf{C_{max}/N}$ will grow, and the peak will become **sharper**, converging towards the theoretical **logarithmic singularity** (divergence) predicted in the thermodynamic limit ($n \to \infty$).
- **Figure B ($\mathbf{C_{max}/N}$ vs. $\ln(\mathbf{n})$):** This plot verifies the $\mathbf{Finite - Size\ Scaling}$ (**FSS**) relation for the 2D Ising Model:

$$\mathbf{C_{max}/N} \sim \ln(\mathbf{n})$$

By plotting the maximum specific heat per spin ($C_{\max}/N$) against the natural logarithm of the lattice dimension ($\ln(n)$), the simulation data should fall onto a **linear trend**, confirming that the simulation correctly captures the critical scaling behavior governed by the critical exponent $\alpha = 0$ (corresponding to logarithmic divergence).

[2] [3]

Contributions

Everybody contributed equally. We helped each other in explaining how to compile and run stuff and verified the results obtained by each of us.

References

[1] A. Zunger and S.-H. Wei, "First-principles studies of ordering and phase separation in semiconductor alloys," *MRS Bulletin*, vol. XV, no. 7, pp. 31–37, 1990.

[2] D. P. Landau and K. Binder, *A Guide to Monte Carlo Simulations in Statistical Physics*. Cambridge University Press, 4th ed., 2009.

[3] S. Arakawa and K. Tanaka, "Monte carlo simulation of the 2d ising model using the metropolis algorithm," *arXiv preprint arXiv:0803.0217*, 2008.

Table 2: Convergence of Cu_3Au $L1_2$ Structure from Three Initial Configurations.

Start No.	Initial a (Å)	Perturbation	Final a (Å)	Final Shape	E_{final}/atom (eV/atom)
1	3.876 (+2% Exp)	Ideal Pos.	**3.625845**	Cubic	−4.274063
2	3.724 (-2% Comp)	Jiggled Pos.	**3.551672**	Cubic	**−4.403313**
3	3.800 (Ideal V)	Light Shear (Normal)	**3.592598**	Cubic?	−4.091665